Computational and Structural Biotechnology Journal 21 (2023) 2837–2844

Contents lists available at ScienceDirect

Computational and Structural Biotechnology Journal

journal homepage: www.elsevier.com/locate/csbj

Research article

On a mechanistic impact of transmembrane tetramerization in the pathological activation of RTKs

Anton A. Polyansky [a,*], Roman G. Efremov [b,c,d]

[a] Department of Structural and Computational Biology, Max Perutz Labs, University of Vienna, Campus Vienna BioCenter 5, A-1030 Vienna, Austria
[b] Shemyakin-Ovchinnikov Institute of Bioorganic Chemistry, Russian Academy of Sciences, 16/10 Miklukho-Maklaya St., 117997 Moscow, Russia
[c] National Research University Higher School of Economics, 20 Myasnitskaya St., Moscow 101000, Russia
[d] Moscow Institute of Physics and Technology (State University), Dolgoprudny, Moscow region, 141701, Russia

ARTICLE INFO

Article history:
Received 14 October 2022
Received in revised form 19 April 2023
Accepted 20 April 2023
Available online 23 April 2023

Keywords:
Pathological mutations
Structure prediction
Molecular dynamics simulations
Signal transduction
Protein oligomerization
Model membranes

ABSTRACT

Constitutive activation of receptor tyrosine kinases (RTKs) via different mutations has a strong impact on the development of severe human disorders, including cancer. Here we propose a putative activation scenario of RTKs, whereby transmembrane (TM) mutations can also promote higher-order oligomerization of the receptors that leads to the subsequent ligand-free activation. We illustrate this scenario using a computational modelling framework comprising sequence-based structure prediction and all-atom 1 μs molecular dynamics (MD) simulations in a lipid membrane for a previously characterised oncogenic TM mutation V536E in platelet-derived growth factor receptor alpha (PDGFRA). We show that in the course of MD simulations the mutant TM tetramer retains stable and compact configuration strengthened by tight protein-protein interactions, while the wild type TM tetramer demonstrates looser packing and a tendency to dissociate. Moreover, the mutation affects the characteristic motions of mutated TM helical segments by introducing additional non-covalent crosslinks in the middle of the TM tetramer, which operate as mechanical hinges. This leads to dynamic decoupling of the C-termini from the rigidified N-terminal parts and facilitates more pronounced possible displacement between the C-termini of the mutant TM helical regions that can provide more freedom for mutual rearrangement of the kinase domains located downstream. Our results for the V536E mutation in the context of PDGFRA TM tetramer allow for the possibility that the effect of oncogenic TM mutations can go beyond alternating the structure and dynamics of TM dimeric states and might also promote the formation of higher-order oligomers directly contributing to ligand-independent signalling effectuated by PDGFRA and other RTKs.

1. Introduction

Receptor-tyrosine kinases (RTKs) undergo dimerization or higher-order oligomerization while performing their functions [27,28,41]. Although, the biochemistry and biophysics of RTK dimerization is under constant scrutiny by the scientific community, the biophysical aspect of their operation and its direct impact on receptor activation is far from being fully understood, especially in the context of oncogenic processes and other functional disorders. For instance, platelet-derived growth factor receptor alpha (PDGFRA), is aberrantly activated in many neoplasms (e.g., glioblastoma), where its pathologic activation is caused by gene amplification, gene fusion, autocrine production of the ligand or point mutations [3,12]. We have previously shown that V536E substitution in the PDGFRA transmembrane (TM) domain is sufficient to constitutively activate the receptor [40]. Moreover, isolated TM domains of the V536E variant were experimentally observed to have a marked tendency to form oligomers of higher order than dimers. The latter was confirmed by SDS PAGE and characteristic NMR spectra for different protein-to-lipid ratios [29]. Meanwhile, oligomerization was impaired for the TM domain of the wild type (WT) protein, for which only a moderate dimerization tendency was detected using the same methods. One reasonable hypothesis in this case could be that the oncogenic V536E mutation modulates the receptor activity by shifting the equilibrium toward the formation of higher-order oligomers, which subsequently facilitates ligand-free activation via increasing the probability of autophosphorylation of kinase domains. First, oligomers promote a higher local concentration of the

* Corresponding author.
E-mail address: anton.polyansky@univie.ac.at (A.A. Polyansky).

https://doi.org/10.1016/j.csbj.2023.04.021

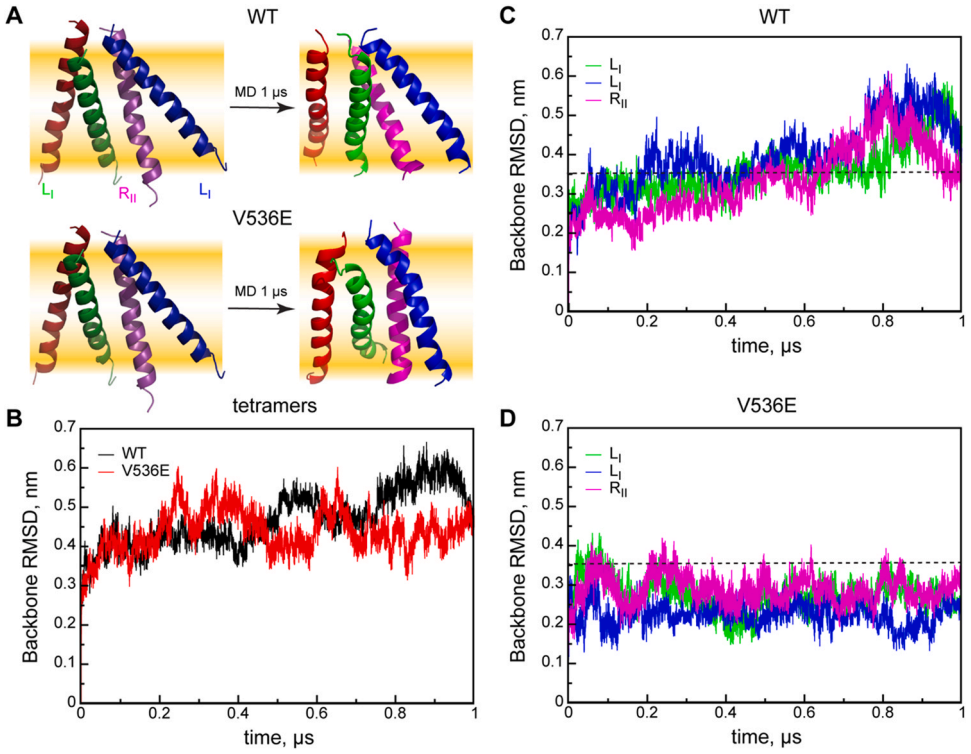

Fig. 1. Evolution of tetrameric configurations during 1 μs MD. **A**. Starting (*left*) and final (*right*) conformations of WT (*up*) and V536E (*bottom*) tetramers from the side view. TM helices are shown in cartoon representation and coloured as follows: red and green – the first left-handed dimer (L_I); magenta and blue – the second left-handed dimer (L_I). The central right-handed dimer (R_{II}) is formed by the green and magenta helices. The POPC lipid bilayer is schematically shown as orange gradients. **B.** Backbone root-mean-square deviations (RMSD) from the initial state of the tetrameric conformation during 1 μs MD simulations for the WT (black) and V536E (red). **C.** Backbone RMSDs from the initial state for individual dimers within the WT tetramer structure the first (green) and second left-handed dimers (blue), as well as the right-handed dimer (magenta). RSMD value of 0.5 nm is indicated with a dashed line. **D.** Backbone RMSDs from the initial state for individual dimers within the V536E tetramer structure. The colour code is the same as in panel C.

catalytic domains. Second, oligomer geometry and dynamics can potentiate the asymmetric arrangement and association of the kinase domains even in the absence of the signal. Thus, basal activation of the homologues PDGFRB receptor can be accomplished via TM domain hetero-oligomerization in the presence of oncoprotein E5 from bovine papillomavirus [19]. Integrin-mediated constitutive activation has been demonstrated for PDGFRB [37,38], whereby β1-integrin and PDGFRB clustering was associated with tyrosine phosphorylation of the receptor [38]. Although at this time the possibility for the PDGFRA receptor to form higher-order oligomers has not been established with certainty, such a capacity was observed for other RTKs, e.g. for ephrin receptors [27,28] or epidermal growth factor receptor (EGFR). Furthermore, ligand-free and ligand-induced oligomerization of EGFR has been shown to be linked to autoinhibition [42] or transition to the fully-activated state [9,10] of the receptor and the formation of signalling platforms characterised by enhanced ('superstoichiometric') response to EGF stimulation [24].

Noteworthily, not only RTKs but many others membrane proteins effectuate their function by directly binding to each other and interacting via different domains including the TM ones. Therefore, understanding the mechanism of TM helix oligomerization would be of general interest. However, experiential studies of TM domains are laborious and are additionally hindered in that highly heterogenous membrane environments are hard to mimic in vitro and to control in vivo. Recent advances in biophysical techniques based on Förster resonance energy transfer enable in vivo studies of signalling and dynamics of membrane protein association specific to different membrane microdomains using specific fluorescent biosensors [44]. Such experiments highlight the importance of receptor localization in a specific membrane environment and/or oligomerization for signal transduction through the membrane to take place. For instance, particularly in the case of RTKs, TM domains gain novel characteristics upon dimerization, which are absent at the monomeric stage (e.g., [32]). Thus, TM dimers can adopt different functional states, and transitions between them usually underlie the protein functioning (see [20] for a recent review). Although a number of studies over the last decade are focused on structure and dynamics of TM dimers and the corresponding protein functions (e.g., active/inactive RTK dimers [7,13]), many questions still remain unanswered. In RTKs, exact allosteric pathways await mapping, and contribution of specific dynamics of TM helices to signal transduction between the receptor and kinase domains requires clarification. Even much less is known about the dynamics and structural organization of higher-order TM oligomers, e. g., tetramers, in which case the key question is the same one asked concerning dimers: does a tetramer resemble a simple sum of its components (TM monomers and dimers) or does tetramerization, as a result of synergy, impart novel properties to the system, which are absent at the level of monomers and dimers? Answering this fundamental question is crucial to understanding the molecular background of cellular signalling, etc., while atomistic modelling in combination with current biophysical techniques are able to provide an efficient research framework suited to such a task, as was previously shown for PDGFRA [29].

In the present study we use different modelling techniques to study the effect of V536E mutation in the context of TM tetramers in comparison to the WT. To this end, we reconstruct the TM tetramer architecture for both variants using a dimer assembly prediction-based approach with recourse to the PREDDIMER web-server [29,30], and explore their structural and dynamic organization in a model lipid membrane in 1 μs all-atom molecular dynamics (MD) simulations. To illustrate the potential biological relevance of the proposed PDGFRA TM tetramer configuration and its realistic membrane topology, we model the putative tetrameric arrangement

of the full-length PDGFRA receptor by fitting MD-derived dimer conformation of the full-length WT PDGFRA dimers in a ligand-free state [31] into the MD-derived TM-tetramer structure.

2. Methods

2.1. Reconstruction of tetrameric configuration for PDGFRA TM

TM sequence fragment ^{522}-SELTVAAAVLVLLVIVIISLIVLVVI-WKQ-^{551} of human PDGFRA (Uniprot ID: P16234) was used for WT and V536E mutant, wherein the corresponding substitution (V- > E) was applied at 536th position. Left-handed (L_I^N) and right-handed (R_{II}^C) TM dimer configuration (Fig. 1**A**) were obtained using the PREDDIMER web-server [30] and combined into a tetrameric arrangement as described also elsewhere [29].

2.2. MD simulations

All MD simulations were performed using GROMACS 4.5 package [33] and Amber99SB-ILDN force-field [21] with the Slipids lipid parameters [17] and TIP3P water model [18] using a protocol similar to the one described elsewhere [17,29]. The initial configurations of the WT and V536E systems were obtained using the *genbox* utility from GROMACS by inserting reconstructed tetramer conformations into a pre-equilibrated 1-palmitoyl-2-oleoyl-sn-glycero-3-phosphocholine (POPC) lipid bilayer comprising 200 molecules (7×7x12 nm^3 box). The final systems each contain 1 protein, 129 lipids, ~14 10^4 water molecules. These systems were energy minimized and subjected to a few steps of MD equilibration with position restraints applied to protein heavy atoms along the X and Y axes. Equilibration steps were performed in different thermodynamic ensembles and using a gradually increasing integration time step: 5000 steps / 0.5 fs / NVT, 25,000 steps / 0.5 fs / NPT semi-isotropic pressure (Berendsen barostat [5]), 250,000 / 1 fs / NPT (Parrinello-Rahman barostat [26]). Finally, production runs of 1 μs were carried out for both systems using a 2 fs time step. A twin-range (0.10 / 0.14 nm) spherical cut-off function was used to truncate van der Waals interactions. Electrostatic interactions were treated using the particle-mesh Ewald summation (real space cutoff 1.0 and 0.12 nm grid with fourth-order spline interpolation). 1 μs MD simulations were carried out using 3D periodic boundary conditions in the isothermal–isobaric (NPT) ensemble with the semisotropic pressure of 1.013 bar for both directions and at a constant temperature of 310 K. The pressure and temperature were controlled during the 1 μs production runs using Nose-Hoover thermostat [16] and a Parrinello-Rahman barostat [26] with 0.5 and 10 ps relaxation parameters, respectively, and a compressibility of 4.5×10^{-5} bar^{-1} for the barostat for both directions. During the simulations the box sizes were adjusting and equilibrating around the following dimensions: to $6.7 \times 6.7 \times 13.2$ nm^3. Protein, lipids and solvent molecules were coupled separately. Bond lengths were constrained using LINCS [15].

2.3. MD analysis

All analyses were done using utilities from the GROMACS 5 package [1] and Linux scripts specially written for this purpose. The following MD-derived parameters were calculated using GROMACS utilities: root-mean-square deviation from the starting configuration and a reference MD trajectory (RMSD, *rms*), radius of gyration (*Rg*, *gyrate*), MD distances between pairs of atoms (*pairdist*). A number of van-der-Waals contacts between protein residues was calculated with the 0.35 nm cut-off value for any interatomic distances between the two moieties. Clustering of MD tetramer conformations was performed using backbone RMSD cut-off defining the cluster perimeter ranging between 0.05 and 0.15 nm with a 0.02 nm step (Fig. S1). An optimal cut-off value of 0.1 nm was selected for further analysis. The characteristic tetramer dynamics were studied using calculations of eigenvectors from mass-weighted variance-covariance matrices obtained for MD distribution of x-, y-, z- atomic degrees of freedom (*covar*). 1μs MD trajectories were filtered (*anaeig*) along the first three eigenvectors (1–3, *anaeig*) and further used for the visualization of TM helix dynamics of and calculations of atomic fluctuations (root-mean-squared fluctuation, RMSF, *rmsf*) corresponding to these components. Pairwise dynamic coupling between protein residues was calculated using the mutual information (MI) formalism applied to protein internal degrees of freedom (bonds-angles-torsions) as it is implemented in the PARENT software [14]. Here. coupling between two residues expressed in terms of the mutual information was calculated from comparison distribution of the corresponding degrees of freedom. Thus obtained all-to-all MI matrices were further used to identify clusters of coupled residues (informational clusters) via agglomerative clustering algorithm [43] with a number of clusters equals to 3. All structures were visualized using Pymol [36].

2.4. Reconstruction of full-length PDGFRA tetramer

The dominant configuration of WT TM tetramer (top cluster, Fig. S1D) and corresponding POPC bilayer configuration (time point 0.5275 μs) were used for fitting representative conformation dimer (top cluster, 18 % occupancy, cut-off 0.3 nm) of the full-length receptor (aa 36–972) in POPC bilayer obtained in all-atom microsecond MD simulations using the same MD protocol as described above [31]. The initial full-length tetramer configuration was assembled in Pymol by fitting the TM regions of the full-length dimer conformation to the TM tetramer structure. The full-length tetramer structure was energy minimized, inserted into equilibrated POPC bilayer (see above) and solvated. The final system size is 16×23×22 nm^3 and this system includes 4 full-length PDGFRA, 1214 POPC, 100 Na+, and ~2×10^5 water molecules. The system was energy minimized and subjected to a few steps of MD equilibration as described above. The full-length tetramer configuration used for illustration obtained after short 1 ns MD production run.

3. Results

3.1. PDGFRA TM domains are able to exist in a tetrameric configuration

Analysis of different dimer conformations possible for PDFGRA TM revealed two dimerization interfaces located on the opposite sides of the helix [29]. While the left-handed dimers for the mutant and WT have very similar configuration, in which helices are associated via interface I of the N-terminal parts (it contains the mutated V536, L_I^N-dimer), the right-handed dimers are different for the two variants. A unique feature of the mutant TM is the ability to form a relatively stable right-handed dimer, in which helices associate along interface II in the C-terminal region (R_{II}^C-dimer). This gives the mutant TM helices the possibility to attain a tetrameric configuration, wherein the R_{II}^C-dimer constitutes the core, while additional helices associate along interface I engaging E536 for interhelical contacts, which results in the formation of two additional L_I^N-dimers. Such a configuration is in agreement with NMR data obtained for the V536E mutant at lower detergent-to-protein ratio [29]. Thus, both the WT and the V536E mutant TM-tetramers were built in the same described configuration (Fig. 1**A**) and subjected to all-atom MD simulations in a POPC lipid bilayer (see below). Interestingly, the L_I^N-dimer represents a conservative TM configuration and was also described for PDGFRB [22]. A potential scenario for receptor tetramerization can be that at first it forms dimers where TM helices adopt L_I^N-configurations and later these dimers interact subsequently with each other and form additional R_{II}^C-dimer at the interface. A similar scenario albeit without higher-order

oligomerization in the TM domain was proposed for the tetramerization of EGFR [24].

3.2. V536E forms stable and converged tetramer configuration in MD

During MD simulations both tetramers display rearrangement of the initial configuration, as is evidenced by root-mean-square deviation (RMSD) from the initial state calculated for backbone atoms (Fig. 1**B**). RMSD for the WT tetramer is gradually increasing up to 0.6 nm and then decreases to 0.5 nm at the very end of the simulation. In contrast, the evolution of V536E tetramer apparently assumes a forward-and-back pattern and mostly remains below 0.5 throughout the trajectory. The mutant tetramer preserves the overall initial configuration (Fig. 1**A, D**), wherein two L_I^N dimers and the central R_{II}^C dimer display RMSD below 0.35 nm during the entire MD trajectory. In the WT tetramers, on the other hand, the helices failed to retain stable arrangement. For instance, one of L_I^N dimers (blue/magenta helices in Fig. 1**A, D**) in WT tends to unfold, as its helices lose their contacts in the N-terminal region and the first helix (blue) forms a new dimer via its N-terminal portion with another partner, while the second one (magenta) only stays in contact with other helices via the C-terminal part (Fig. 1**A**). The V536E mutation stabilizes the left-handed dimers along interface I and facilitates the formation of a stable R_{II}^C dimer that directly contributes to the stability and structural organization peculiar to the mutant tetramer. Detailed structural cluster analysis of tetrameric configurations (Fig. S1) reveals convergence-type behaviour for the mutant, insofar as its conformation is gradually evolving (Fig. S1B) toward the dominant state observed during the final part of the MD trajectory shown in Fig. S1C (a structure representative of the most occupied structural cluster 1 with the occupancy of 17.2 %). This convergence of the tetrameric configuration is evident in the decreasing mutual RMSD values between the representative structures from top three clusters (Fig. S1D). In contrast, for the WT tetramer the dominant conformation (cluster 1, 16 %) forms in the middle portion of the MD trajectory and goes on to evolve into a less populated state (cluster 2, 9.8 %), unstable towards the end of the simulations. This evolution is characterized by gradually increasing RMSD values between representative conformations of top three clusters along the trajectory (Fig. S1D). Importantly, the mutant tetramer remains tightly packed during MD with a tendency towards further compaction (Fig. 2**A, B**), whereas the WT helical bundle opens up to accommodate lipid molecules in the tetramer interior (Fig. 2**A, B**). Thus, the number of protein-protein contacts remains stable for the mutant tetramer during MD and is almost halved for the WT (Fig. 2**C**). The latter clearly indicates a transient nature of the WT tetramer with a tendency to dissociate. Meanwhile, compact organization of the mutant bundle with the well-preserved configuration of both L_I^N dimers facilitates wider lateral separation between the C-termini compared to WT (Fig. 2**D**). Importantly, in dimers intermediate separations of their C-termini are much higher populated than the tetrameric state and the long-range separation distances were not observed (Fig. S2A).

3.3. V536E mutation decouples dynamics of N- and C-termini within the tetramer

Transmission of allosteric signal between the receptor and kinase parts of RTKs assumes a presence of a characteristic pattern in the dynamics of TM helices, whereby different perturbation in its N-terminal parts is directly transmitted towards the C-termini. Hence, the dynamic effect of the mutation was investigated in the context of a tetramer. The principal component analysis of MD-derived covariance matrices demonstrates a marked difference between the dynamics in the WT and mutant tetramers. While only the first 10 eigenvalues obtained differ substantially between the two systems, the first 3 eigenmodes cover about 60 % of the statistical variation in WT and somewhat less in V536E, approx. 50 %. (Fig. 3**A**). Analysis of coordinate variances during MD associated with the corresponding eigenvectors (or RMSF values for MD trajectories filtered along the first 3 eigenvectors) clearly demonstrates different dynamic patterns along TM helices in WT and mutant tetramer (Fig. 3**B**). WT helices accumulate most of the dynamics in the N-terminal portions, while in the mutant this effect shifts towards the C-termini, which display the highest mobility, while the rest of the mutant tetramer is relatively rigid (Fig. 3**C**). The dynamic difference between the WT and mutant is clearly seen in a visualization of MD trajectories filtered along the first 3 principal components (Movie S1, S2). WT helices demonstrate piston-like movements as the bundle drifts towards falling apart (Movie S1). Meanwhile, mutant helices move with a smaller amplitude, with most of the dynamics manifested in the C-terminal part (Movie S2). Interestingly, the mutant helices lose translational freedom and look “glued” around the middle portion by polar Glu sidechains. The latter affects intercommunication between the helices and their dynamic coupling (see Methods). Thus, the information clusters for the tetramers include all 4 helices, whereby it can be observed clear decoupling between the N- and C-regions for the mutant (two separate information clusters, Fig. S2B).

Supplementary material related to this article can be found online at doi:10.1016/j.csbj.2023.04.021.

4. Discussion

The results of the modelling of the two variants of the PDGFRA TM tetramer could offer certain potential mechanistic explanations of constitutive receptor activation via oligomerization induced by the oncogenic mutation, which are summarized in Fig. 4. To illustrate potential biological relevance of proposed PDGFRA TM tetramer configuration and its realistic membrane topology we model putative tetrameric arrangement of the full-length PDGFRA receptor (Fig. 4**,** see Methods for the details). The tetramer configuration accommodates two full-length dimers without any sterical clashes and preserves their realistic membrane topology. This WT full-length tetramer configuration represents a transient association between two corresponding dimers via interactions between kinase and TM domains. Moreover, in the case of WT, TM helices are able to form a dimeric configuration (presumably, L_I^N-dimer) that corresponds to the inactive state of the receptor as suggested before [29],while the subsequent oligomerization step is hindered due to the observed transient nature and instability of the tetrameric state. Therefore, in the absence of the ligand (PDGF), WT PDGFRA most likely remains in inactive dimeric states, in which it can only be activated upon ligand binding and the ensuing allosterically induced rearrangement of TM helices into the active configuration. Importantly, both in the WT dimers [29] and the WT tetramer the helices demonstrate translational piston-like motions and fully-coupled disposition of their N- and C-terminal parts suggesting that the mutual arrangement of the C-termini can only be modulated simultaneously with those of the N-termini (see Movie S1). The introduction of polar Glu residue in the middle of the PDGFRA TM helix as a result of the phenotypic mutation affects both the oligomerization of the mutant TM domains and their characteristic dynamics. The V536E mutant has been shown to enter a stable tetrameric state, which in its turn may represent a nucleation step for subsequent oligomerization. Indeed, pre-formed mutant tetramers can further associate along the exposed R_{II}^C interfaces, initiating a chain process, which would be limited by concertation of the receptor and leads to increasing effective concertation of the kinase domains in local proximities. This by itself can increase the chance of spontaneous formation of their active configurations. The oligomerization potential of isolated V536E TM domains was previously observed experimentally [29], with a tendency to form a tetrameric state and move on to the next

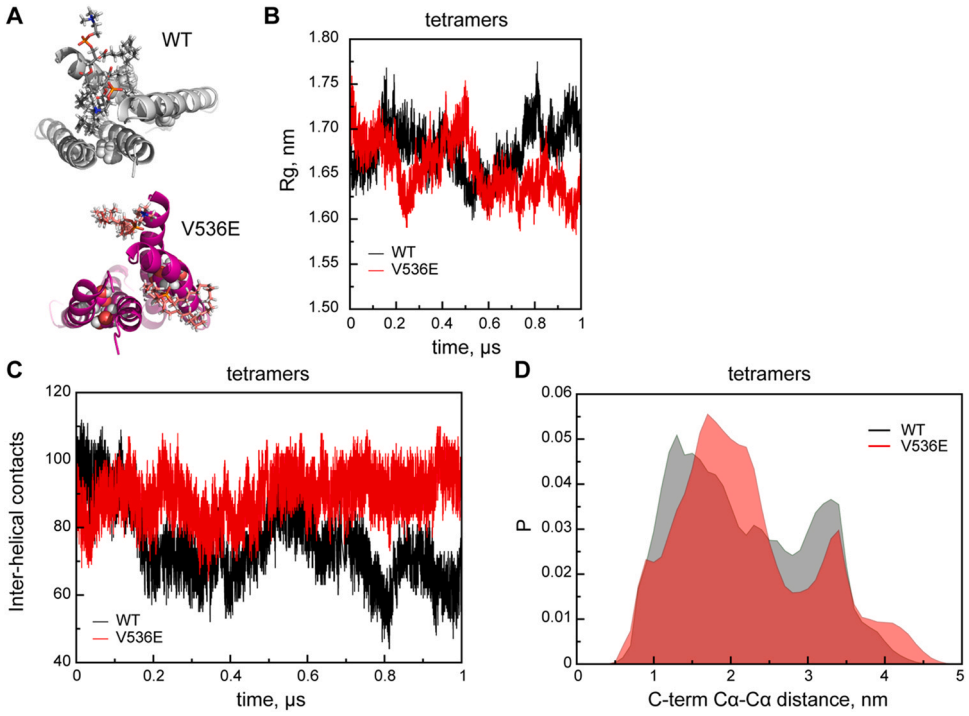

Fig. 2. Tetramer packing and mutual arrangement. **A.** Final snapshots of the WT (coloured grey) and the V536E (coloured magenta) tetramers viewed from the top and shown in cartoon representation with the closest lipid neighbours in stick representation. **B**. MD evolution of the radius of gyration (*Rg*) calculated for tetramer conformations of the WT (black) and V536E (red). **C**. The total number of inter-helical atomic protein contacts for the WT (black) and V536E (red) tetramers. **D.** MD distributions of pairwise distances between Cα-atoms of the C-terminal residues in the WT (dark grey) and V536E (red) tetramers.

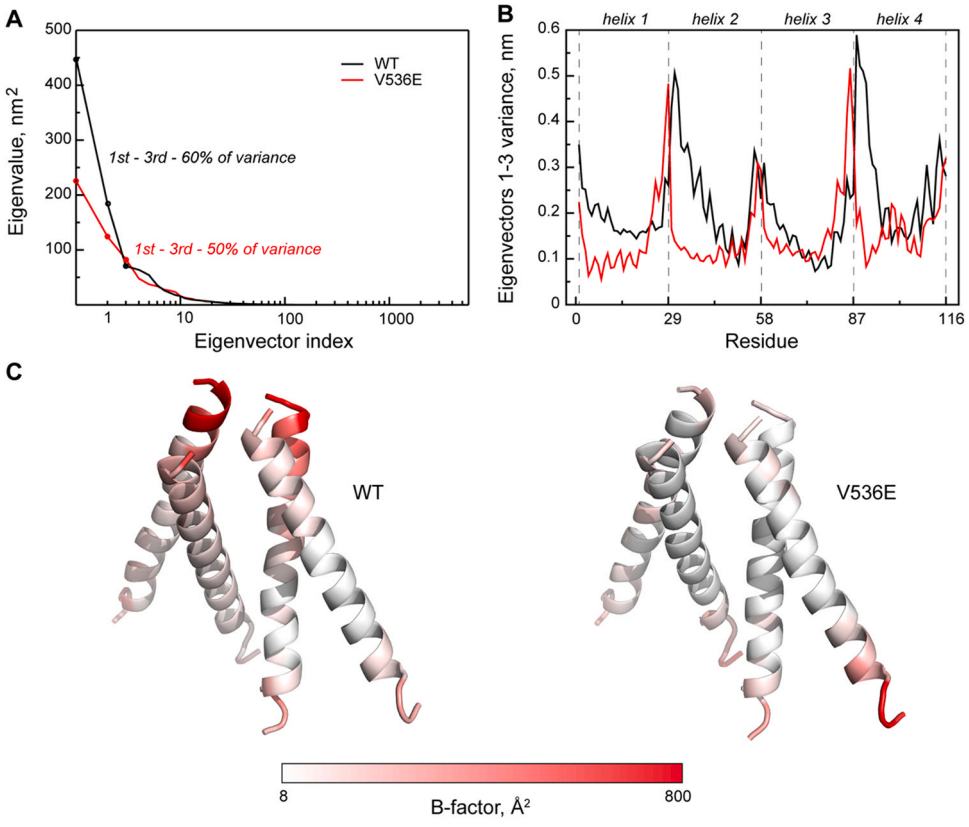

Fig. 3. Characteristic dynamics of TM helices in tetrameric configuration. **A.** Distributions of eigenvalues for the mass-weighted MD covariance matrix for WT (black) and V536E (red) tetramers. First three eigenvalues are shown as filled circles. **B**. Sequence profiles of per residue atomic root-mean-square fluctuations (RMSF) along the first three eigenvectors for WT (black) and V536E (red) tetramers. Regions corresponding to individual TM helices are designated with vertical dashed lines. **C**. 3D distribution of atomic RMSFs along the first three eigenvectors in the tetramer structures of the WT (*left*) and V536E (*right*). Tetramers are shown in cartoon representation. Helices are coloured in accordance with the corresponding B-factor scale presented below the panel.

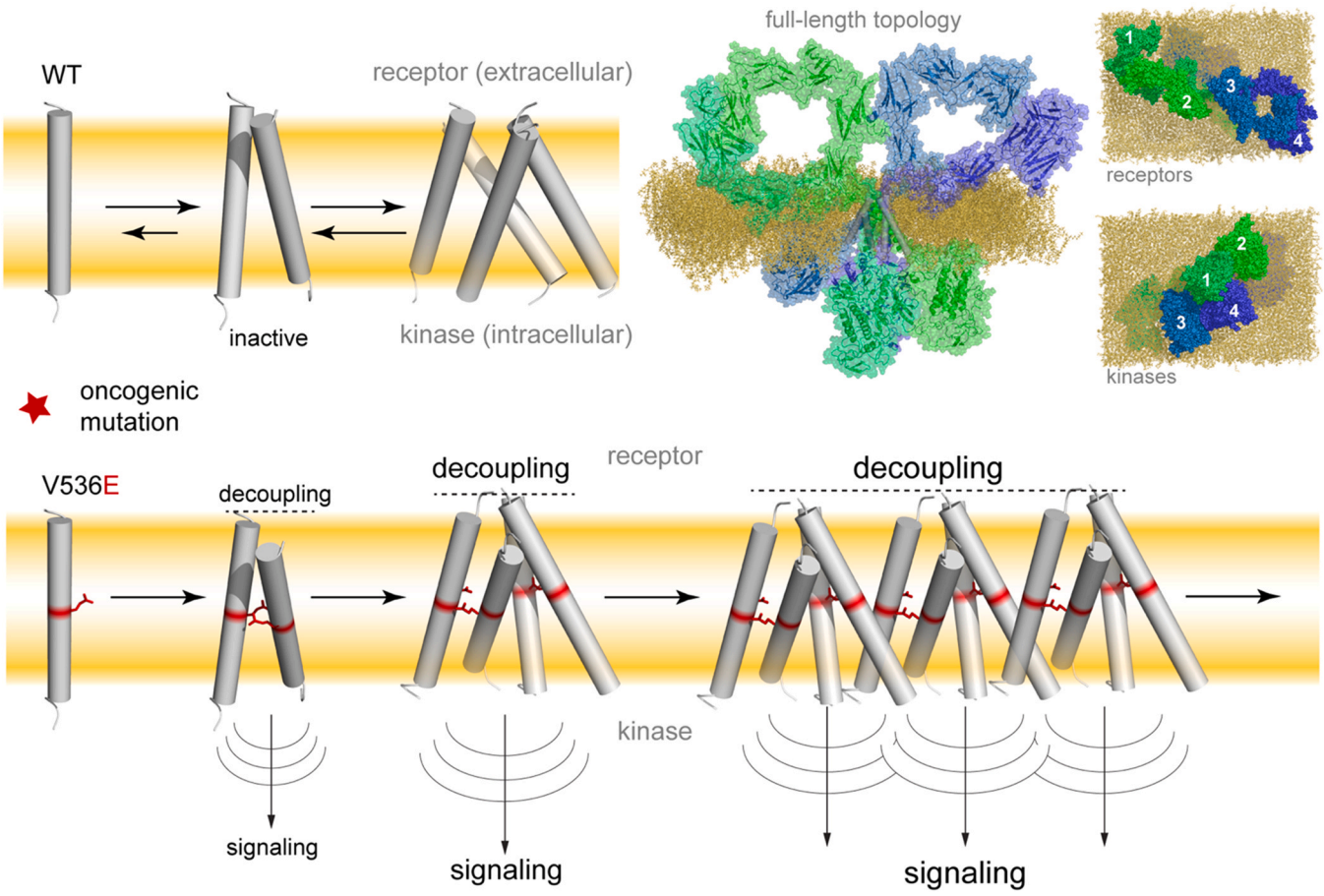

Fig. 4. The hypothetical scheme of PDGFRA activation via TM oligomerization. WT TM domains have low tendency for dimer formation and further oligomerization is hindered (*top panel*). The corresponding putative membrane bound tetrameric arrangement of the full-length PDGFRA receptor is shown in the right corner, whereby POPC lipids are shown with lines, the receptor monomers are shown with spheres and cartoon representation and coloured in shades of green (first dimer) and blue (second dimer) colours. Isolated TM tetramer configuration is fitted to the full-length oligomer and shown with grey cylinders. In lateral view lipids in front were removed for clarity. In top and bottom views individual monomers are indicated with white numbers. Oncogenic mutation (e. g. V536E, shown as red sticks) promotes TM domain oligomerization and subsequent activation, during which the tetramer represents a building block in chain oligomerization (*bottom panel*).

iteration of the suggested oligomerization pathway (e.g., octamers). Moreover, much like the dimer [29] the mutant TM tetramer, a "building block" in high-order oligomerization, demonstrates a dynamic pattern characterised by alternated decoupling between the N- and C-termini due to the presence of non-covalent Glu crosslinks in the middle part. More specifically, changes in the configuration of the C-terminal portions can occur independently of those in the N-terminal ones in the absence of any allosteric impulse (see Movie S2, Fig. S2B). As has been shown, the C-terminal parts are indeed the most dynamic regions in the tetramer and display considerable mutual displacement that in context of the full-length receptor would give more freedom for downstream kinase domains to undergo potential rearrangement into asymmetric configurations initiating autophosphorylation and initiate the subsequent signalling cascade.

Our results give a novel perspective for potential biomedical applications and can be used as a starting point in the development of new drugs and therapeutic strategies to control PDGFRA functioning and to combat pathologies caused by its dysfunction. At the same time, we should highlight an important fundamental aspect of the presented data and conclusions. In the particular case of PDGFRA, it was shown for the first time that for single-pass membrane proteins (RTKs, etc.), knowledge of the molecular basis of their TM dimerization may not be sufficient to understand the functioning of the receptor(s) within the living cell, if it involves higher-order oligomerization, e. g. the formation of tetramers. Thus, within the presented mechanistic framework it is shown that the structure and dynamics of the tetramer can radically differ from the properties of their two constituent dimers pointing toward synergy in the behaviour of the system should its oligomeric state change. In addition, comparative analysis of TM domains in the WT and V536E mutant revealed a fundamental difference in the behaviour of the system as a whole, mainly due to drastic changes in the corresponding dynamics of TM helices. Such effects are hard to detect only using modern instrumental methods, but based on *in silico* prediction, experiments can be planned to create and test new mutant forms of RTK with specified properties.

It is important to note that a number of additional factors also contributing to PDGFRA oligomerization are beyond the scope of the present study, which mainly focuses on the receptor TM domains. Better understanding of the possible structural organisation of PDGFRA oligomers and effectuation of the receptor functional dynamics in that context might require taking into account RTK juxtamembrane regions, receptor or/and kinase domains, and, at best, the full-length receptors for the future detailed investigation. While for EGFR all-atom MD simulations of full-length receptor dimers [4] or oligomers of their receptor portions [42] have already been performed, in the case of PDGFRA equivalent studies still remain to be undertaken, which we are focusing on at this moment. Certain important aspects of the structural and dynamic behaviour of RTKs' TM domains were not addressed in the aforementioned studies. Neither have the effects of pathogenic point mutations been considered in a

comparison to WT proteins. Another aspect is the potential role of the membrane environment in receptor oligomerization. As was shown in the case of PDGFRB [37] and other receptors, their clustering and activation can be controlled by placing them in a specific membrane environment (e.g. lipid rafts) [8,35].

The proposed mechanism of PDGFRA constitutive activation via TM mutation-induced chain oligomerization offers an interesting perspective in the understanding of the initial stage of RTK-related disorders. While being hypothetical this mechanism requires direct experimental validation in vivo, which may be laborious due to limited resolution and a number of known experimental biases (e. g., receptor overexpression typical for such experiments). At the same time, oligomerization-driven development of pathological states due to a single-point mutation in the PDGFRA TM domain relates this process to other known phenomena of this kind e.g., neurodegenerative diseases in the course of which single-point mutations often lead to pathological protein aggregation [6,25,34,39]. Interestingly, it has recently been shown that human disease-related mutations are also more likely to increase protein aggregation than non-disease-related ones, and it has been suggested that disease-associated protein aggregation is quite a widespread phenomenon [11]. Thus, putative mechanism of PDGFRA activation via the oligomerization-prone TM mutation may be one occurrence of a universal principle underlying different human pathologies.

5. Conclusion

In this study we investigate a hypothetical RTK activation mechanism due to TM mutations associated with higher-order receptor oligomerization. Based on the configuration predicted for the PDGFRA TM tetramer we demonstrate that the V536E mutant tetramer retains stable configuration in microsecond-range MD simulations, while WT tetramer displays a clear tendency to dissociate. Apart from tetramer stability, V536E alternates the dynamics of TM helices within the tetrameric arrangement. Specifically, WT helices within the tetramer perform piston-like motions en bloc, restricting lateral displacement of the C-termini and their mobility, while the mutant helices demonstrate increased mobility in the C-terminal parts, which is also decoupled from more constrained N-termini. Among the new interesting results of this work is that the structure and dynamics of RTKs' tetramers can be significantly different from those of their dimers. Such synergy may play an important functional role in cell signalling. By synergy we assume getting novel properties or characteristics, which are absent in isolated dimers. Here, tetramerization leads to formation of a unified allosterically coupled system and not just to a simple sum of the disconnected dimers. The results of atomistic modelling allow one to observe the potential impact of higher-order receptor oligomerization induced by TM mutation on ligand-independent signalling of PDGFRA, which may also be relevant to other members of the RTK family. This constitutes a potentially new layer in constitutive receptor activation and may stimulate search for novel biomedical applications. While targeting TM domains of single-pass membrane receptors and modulating their dimerization and subsequent activation represents a promising therapeutic concept (e.g., "interceptor" peptides [2,23,41]), the putative activation scenario proposed here for RTKs might form the basis for the development of medical strategies to specifically inhibit and prevent pathological oligomerization in the TM region.

CRediT authorship contribution statement

Anton A. Polyansky & Roman G. Efremov: Conceptualization, Methodology, Writing- Reviewing and Editing. Anton A. Polyansky: Data curation, Writing- Original draft preparation, Visualization, Investigation. Roman G. Efremov: Supervision.

Conflict of Interest

None.

Acknowledgements

The work was supported by the Russian Science Foundation (grant 23-14-00313 for RGE). Supercomputer calculations were performed within the framework of the HSE University Basic Research Program. Access to computational facilities of the Supercomputer Center "Polytechnical" at the St. Petersburg Polytechnic University is gratefully appreciated.

Appendix A. Supporting information

Supplementary data associated with this article can be found in the online version at doi:10.1016/j.csbj.2023.04.021.

References

[1] Abraham MJ, Murtola T, Schulz R, Páll S, Smith JC, Hess B, Lindahl E. GROMACS: high performance molecular simulations through multi-level parallelism from laptops to supercomputers. SoftwareX 2015;1–2:19–25. https://doi.org/10.1016/j.softx.2015.06.001
[2] Albrecht C, Appert-Collin A, Bagnard D, Blaise S, Romier-Crouzet B, Efremov RG, Bennasroune A. Transmembrane peptides as inhibitors of protein-protein interactions: an efficient strategy to target cancer cells. Front Oncol 2020;10. https://doi.org/10.3389/fonc.2020.00519
[3] Andrae J, Gallini R, Betsholtz C. Role of platelet-derived growth factors in physiology and medicine. Genes Dev 2008;22(10):1276–312. https://doi.org/10.1101/gad.1653708
[4] Arkhipov A, Shan Y, Das R, Endres NF, Eastwood MP, Wemmer DE, Shaw DE. Architecture and membrane interactions of the EGF receptor. Cell 2013;152(3):557–69. https://doi.org/10.1016/j.cell.2012.12.030
[5] Berendsen HJC, Postma JPM, van Gunsteren WF, DiNola A, Haak JR. Molecular dynamics with coupling to an external bath. J Chem Phys 1984;81(8):3684. https://doi.org/10.1063/1.448118
[6] Bertram L, Tanzi RE. The genetic epidemiology of neurodegenerative disease. J Clin Invest 2005;115(6):1449–57. https://doi.org/10.1172/jci24761
[7] Bocharov EV, Bragin PE, Pavlov KV, Bocharova OV, Mineev KS, Polyansky AA, Arseniev AS. The conformation of the epidermal growth factor receptor transmembrane domain dimer dynamically adapts to the local membrane environment. Biochemistry 2017;56(12):1697–705. https://doi.org/10.1021/acs.biochem.6b01085
[8] Bocharov EV, Mineev KS, Pavlov KV, Akimov SA, Kuznetsov AS, Efremov RG, Arseniev AS. Helix-helix interactions in membrane domains of bitopic proteins: specificity and role of lipid environment. Biochim Biophys Acta Biomembr 2017;1859(4):561–76. https://doi.org/10.1016/j.bbamem.2016.10.024
[9] Clayton AH, Orchard SG, Nice EC, Posner RG, Burgess AW. Predominance of activated EGFR higher-order oligomers on the cell surface. Growth Factors 2008;26(6):316–24. https://doi.org/10.1080/08977190802442187
[10] Clayton AH, Walker F, Orchard SG, Henderson C, Fuchs D, Rothacker J, Burgess AW. Ligand-induced dimer-tetramer transition during the activation of the cell surface epidermal growth factor receptor-a multidimensional microscopy analysis. *J Biol Chem, 280*(34), 30392-30399 2005. https://doi.org/10.1074/jbc.M504770200
[11] De Baets G, Van Doorn L, Rousseau F, Schymkowitz J. Increased aggregation is more frequently associated to human disease-associated mutations than to neutral polymorphisms. PLoS Comput Biol 2015;11(9):e1004374. https://doi.org/10.1371/journal.pcbi.1004374
[12] Demoulin JB, Essaghir A. PDGF receptor signaling networks in normal and cancer cells. Cytokine Growth Factor Rev 2014;25(3):273–83. https://doi.org/10.1016/j.cytogfr.2014.03.003
[13] Endres NF, Das R, Smith AW, Arkhipov A, Kovacs E, Huang Y, Kuriyan J. Conformational coupling across the plasma membrane in activation of the EGF receptor. Cell 2013;152(3):543–56. https://doi.org/10.1016/j.cell.2012.12.032
[14] Fleck M, Polyansky AA, Zagrovic B. PARENT: a parallel software suite for the calculation of configurational entropy in biomolecular systems. J Chem Theory Comput 2016;12(4):2055–65. https://doi.org/10.1021/acs.jctc.5b01217
[15] Hess B, Bekker H, Berendsen HJC, Fraaije JGEM. LINCS: a linear constraint solver for molecular simulations. J Comput Chem 1997;18(12):1463–72. doi:Doi 10.1002/(Sici)1096-987x(199709)18:12 < 1463::Aid-Jcc4 > 3.0.Co;2-H.
[16] Hoover WG. Canonical dynamics: equilibrium phase-space distributions. Phys Rev A Gen Phys 1985;31(3):1695–7. Retrieved from http://www.ncbi.nlm.nih.gov/pubmed/9895674.
[17] Jambeck JP, Lyubartsev AP. Derivation and systematic validation of a refined all-atom force field for phosphatidylcholine lipids. J Phys Chem B 2012;116(10):3164–79. https://doi.org/10.1021/jp212503e
[18] Jorgensen WL. Quantum and statistical mechanical studies of liquids.10. transferable intermolecular potential functions for water, alcohols, and ethers -

application to liquid water. J Am Chem Soc 1981;103(2):335–40. doi:DOI 10.1021/ja00392a016.
[19] Karabadzhak AG, Petti LM, Barrera FN, Edwards APB, Moya-Rodríguez A, Polikanov YS, DiMaio D. Two transmembrane dimers of the bovine papillomavirus E5 oncoprotein clamp the PDGF β receptor in an active dimeric conformation. Proc. Natl. Acad. Sci. 2017:201705622. https://doi.org/10.1073/pnas.1705622114
[20] Kovacs T, Zakany F, Nagy P. It takes more than two to tango: complex, hierarchal, and membrane-modulated interactions in the regulation of receptor tyrosine kinases. Cancers 2022;14(4):944. Retrieved from ⟨https://www.mdpi.com/2072-6694/14/4/944⟩.
[21] Lindorff-Larsen K, Piana S, Palmo K, Maragakis P, Klepeis JL, Dror RO, Shaw DE. Improved side-chain torsion potentials for the Amber ff99SB protein force field. Proteins 2010;78(8):1950–8. https://doi.org/10.1002/prot.22711
[22] Muhle-Goll C, Hoffmann S, Afonin S, Grage SL, Polyansky AA, Windisch D, Ulrich AS. Hydrophobic matching controls the tilt and stability of the dimeric platelet-derived growth factor receptor (PDGFR) β transmembrane segment. J Biol Chem 2012;287(31):26178–86. https://doi.org/10.1074/jbc.M111.325555
[23] Najumudeen AK. Receptor tyrosine kinase transmembrane domain interactions: potential target for "Interceptor" therapy. jc6-jc6 Sci Signal 2010;3(138). https://doi.org/10.1126/scisignal.3138jc6
[24] Needham SR, Roberts SK, Arkhipov A, Mysore VP, Tynan CJ, Zanetti-Domingues LC, Martin-Fernandez ML. EGFR oligomerization organizes kinase-active dimers into competent signalling platforms. Nat Commun 2016;7(1):13307. https://doi.org/10.1038/ncomms13307
[25] Nomura T, Watanabe S, Kaneko K, Yamanaka K, Nukina N, Furukawa Y. Intranuclear aggregation of mutant FUS/TLS as a molecular pathomechanism of amyotrophic lateral sclerosis. J Biol Chem 2014;289(2):1192–202. https://doi.org/10.1074/jbc.M113.516492
[26] Parrinello M, Rahman A. Polymorphic transitions in single-crystals - a new molecular-dynamics method. J Appl Phys 1981;52(12):7182–90. doi:Doi 10.1063/1.328693.
[27] Paul MD, Hristova K. The RTK interactome: overview and perspective on RTK heterointeractions. Chem Rev 2019;119(9):5881–921. https://doi.org/10.1021/acs.chemrev.8b00467
[28] Paul MD, Hristova K. The transition model of RTK activation: a quantitative framework for understanding RTK signaling and RTK modulator activity. Cytokine Growth Factor Rev 2019;49:23–31. https://doi.org/10.1016/j.cytogfr.2019.10.004
[29] Polyansky AA, Bocharov EV, Velghe AI, Kuznetsov AS, Bocharova OV, Urban AS, Efremov RG. Atomistic mechanism of the constitutive activation of PDGFRA via its transmembrane domain. Biochim Biophys Acta Gen Subj 2019;1863(1):82–95. https://doi.org/10.1016/j.bbagen.2018.09.011
[30] Polyansky AA, Chugunov AO, Volynsky PE, Krylov NA, Nolde DE, Efremov RG. PREDDIMER: a web server for prediction of transmembrane helical dimers. Bioinformatics 2013;30(6):889–90. https://doi.org/10.1093/bioinformatics/btt645
[31] Polyansky, A.A., Efremov, R.G. (in preparation). Structural organization and allosteric communication of full-length PDGFRA.
[32] Polyansky AA, Volynsky PE, Efremov RG. Multistate organization of transmembrane helical protein dimers governed by the host membrane. J Am Chem Soc 2012;134(35):14390–400. https://doi.org/10.1021/ja303483k
[33] Pronk S, Pall S, Schulz R, Larsson P, Bjelkmar P, Apostolov R, Lindahl E. GROMACS 4.5: a high-throughput and highly parallel open source molecular simulation toolkit. Bioinformatics 2013;29(7):845–54. https://doi.org/10.1093/bioinformatics/btt055
[34] Ross CA, Poirier MA. Protein aggregation and neurodegenerative disease. Nat Med 2004;10(*Suppl*):S10–7. https://doi.org/10.1038/nm1066
[35] Roy A, Patra SK. Lipid raft facilitated receptor organization and signaling: a functional rheostat in embryonic development, stem cell biology and cancer. Stem Cell Rev Rep 2022. https://doi.org/10.1007/s12015-022-10448-3
[36] Schrodinger, L.L.C. (2010). The PyMOL Molecular Graphics System, Version 1.3r1.
[37] Seong J, Huang M, Sim KM, Kim H, Wang Y. FRET-based visualization of PDGF receptor activation at membrane microdomains. Sci Rep 2017;7(1):1593. https://doi.org/10.1038/s41598-017-01789-y
[38] Sundberg C, Rubin K. Stimulation of beta1 integrins on fibroblasts induces PDGF independent tyrosine phosphorylation of PDGF beta-receptors. J Cell Biol 1996;132(4):741–52. https://doi.org/10.1083/jcb.132.4.741
[39] Vance C, Rogelj B, Hortobágyi T, De Vos KJ, Nishimura AL, Sreedharan J, Shaw CE. Mutations in FUS, an RNA processing protein, cause familial amyotrophic lateral sclerosis type 6. Science 2009;323(5918):1208–11. https://doi.org/10.1126/science.1165942
[40] Velghe AI, Van Cauwenberghe S, Polyansky AA, Chand D, Montano-Almendras CP, Charni S, Demoulin JB. PDGFRA alterations in cancer: characterization of a gain-of-function V536E transmembrane mutant as well as loss-of-function and passenger mutations. Oncogene 2014;33(20):2568–76. https://doi.org/10.1038/onc.2013.218
[41] Westerfield JM, Barrera FN. Membrane receptor activation mechanisms and transmembrane peptide tools to elucidate them. J Biol Chem 2020;295(7):1792–814. https://doi.org/10.1074/jbc.REV119.009457
[42] Zanetti-Domingues LC, Korovesis D, Needham SR, Tynan CJ, Sagawa S, Roberts SK, Martin-Fernandez ML. The architecture of EGFR's basal complexes reveals autoinhibition mechanisms in dimers and oligomers. Nat Commun 2018;9(1):4325. https://doi.org/10.1038/s41467-018-06632-0
[43] Zepeda-Mendoza ML, Resendis-Antonio O. Hierarchical Agglomerative Clustering. In: Dubitzky W, Wolkenhauer O, Cho K-H, Yokota H, editors. Encyclopedia of Systems Biology. New York, NY: Springer New York; 2013. p. 886–7.
[44] Zhang J-F, Mehta S, Zhang J. Signaling microdomains in the spotlight: visualizing compartmentalized signaling using genetically encoded fluorescent biosensors. Annu Rev Pharmacol Toxicol 2021;61(1):587–608. https://doi.org/10.1146/annurev-pharmtox-010617-053137